Electronic spectroscopy of 1,3,5,7-cyclooctatetraene by low-energy, variable-angle electron impact[a)]

Robert P. Frueholz[b)] and Aron Kuppermann

Arthur A. Noyes Laboratory of Chemical Physics, California Institute of Technology, Pasadena, California 91125 [c)]

(Received 20 February 1978)

The electron-impact energy loss spectrum of 1,3,5,7-cyclooctatetraene has been measured at electron impact energies of 30, 50, and 75 eV, and scattering angles varying from 5° to 80°. Three transitions with maxima at 3.05, 4.05, and 4.84 eV are identified as singlet → triplet excitations. The significance of the lowest lying of these triplet states in the quenching process of dye laser solutions (in particular rhodamine 6G) is discussed and an exciplex mechanism for triplet quenching is suggested. Singlet→singlet transitions are observed at 4.43, 6.02, and 6.42 eV. These spin-allowed transitions have been observed optically and are assigned as $\tilde{X}\,^1A_1 \rightarrow {}^1A_2$, $\tilde{X}\,^1A_1 \rightarrow {}^1E$, and $\tilde{X}\,^1A_1 \rightarrow {}^1E$ excitations. Three new, singlet → singlet transitions are observed at 6.99, 8.41, and 9.05 eV and are tentatively assigned as the $\tilde{X}\,^1A_1 \rightarrow {}^1B_2$, $\tilde{X}\,^1A_1 \rightarrow {}^1E$, and $\tilde{X}\,^1A_1 \rightarrow {}^1E$, $\pi \rightarrow \pi^*$ excitations. Several superexcited features between 10 and 15 eV have been observed and are believed to involve excitations to autoionizing Rydberg states.

I. INTRODUCTION

The 1, 3, 5, 7-cyclooctatetraene (COT) molecule is an example of a nonaromatic,[1] cyclic, conjugated carbon–carbon double bond system. The ground electronic state, which has been studied by electron diffraction techniques,[2,3] was found to be nonplanar and "tub" shaped. COT exhibits D_{2d} symmetry which may be seen from the following structure,[2]

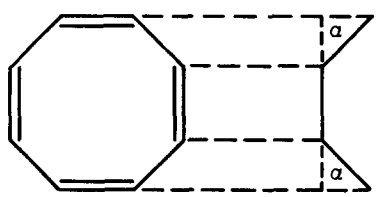

where the C=C, C–C, and C–H bond lengths are 1.340, 1.475, and 1.100 Å, respectively, the C=C–C angle is 126.1°, the H–C=C angle is 117.6°, and α is 43.1°.

Due to its nonplanar structure COT is an interesting molecule regarding σ–π interactions, through-bond interactions, and through-space interactions.[4–7] COT is also an efficient triplet quencher for several dye laser solutions[8–12] (e.g., rhodamine 6G and brilliant sulfaflavine). Moderate concentrations of this molecule (~ 1×10^{-4}M/liter)[11] in ethanol not only increase pulse length but increase the maximum pulse repetition rate of those lasers and also permit cw operation of some of them. One of the aims of the present investigation has been to obtain high-quality electronic band shapes and accurate locations of the intensity maxima for the low-lying singlet → triplet transitions of COT by low-energy, variable-angle, electron-impact spectroscopy. This information should aid in the understanding of the effect of COT as a triplet quencher. A previous trapped electron study[13] has indicated the presence of several triplet excited states in the region from 3 to 4.5 eV and it was further hoped that our experiments would provide more detailed information and a better understanding of this energy-loss region.

II. SUMMARY OF PREVIOUS STUDIES

COT has 56 electrons which, in the ground state, occupy the following set of 28 molecular orbitals[4]: five a_1, two a_2, three b_1, four b_2, and seven doubly degenerate e orbitals. The ordering of the higher occupied molecular orbitals, from which low-lying excitations are expected is somewhat uncertain. Van-Catledge,[7] using the semiempirical INDO formalism, places the highest orbital of each symmetry, with increasing energy, in the order, $4b_2(\pi)$, $3b_1(\sigma)$, $7e(\pi)$, and $5a_1(\pi)$. Batich *et al.*[4] have performed semiempirical MINDO/2 calculations yielding a similar ordering. However, they feel that the $3b_1$ orbital has an erroneously high energy and support this opinion by referring to the *ab initio* results of Lehn and Wipf. The latter found, using several different Gaussian-type orbital basis sets that the $3b_1$ orbital has a lower energy yielding the ordering $3b_1(\sigma)$, $4b_2(\pi)$, $7e(\pi)$, and $5a_1(\pi)$. Electronic transitions are expected to occur from these higher occupied orbitals to the following lower vacant molecular orbitals[7]: $3a_2(\pi)$, $8e(\pi)$, $4b_1(\pi)$, and $5b_2(\sigma)$. Table I summarizes the theoretical results for transition energies. They are all semiempirical, as no *ab initio* values have been published so far. Unfortunately most calculations only consider singlet → singlet transitions; results for singlet → triplet excitations are limited.[13,14]

The optical absorption spectrum of COT[6] shows a broad weak band extending from 4.00 to 4.77 eV with a maximum at 4.39 eV assigned to be the $\tilde{X}\,^1A_1 \rightarrow {}^1A_2$ excitations.[15] In addition, an intense band at 6.42 eV (the upper transition energy limit of the experimental study) is assigned as $\tilde{X}\,^1A_1 \rightarrow {}^1E$, with another $\tilde{X}\,^1A_1 \rightarrow {}^1E$ excitation producing a pronounced inflection at 6.05 eV. Cope and Overberger[16] also observed a weak transition at

a)This work was supported by a Contract (No. EY-76-S-03-767) from the Department of Energy. Report Code: CALT-767P4-163.

b)Work performed in partial fulfillment of the requirements for the Ph.D. degree in Chemistry at the California Institute of Technology.

c)Contribution No. 5732.

 0021-9606/78/6908-3614$01.00

TABLE I. Summary of semiempirical theoretical calculations of transition energies.

Electronic state	Contributing configurations[a]	Symmetry[b] characterization	Calculated Energies (eV) Van-Catledge[c]	Allinger[d]	Allinger[e]	Knoop[f]	Baird[g]
Not designated	$S_0 \rightarrow T_1$					3.41	1.37
Not designated	$S_0 \rightarrow T_2$					3.78	
Not designated	$S_0 \rightarrow T_3$					4.21	
$^1A_2$	$5a_1 \rightarrow 3a_2$	F	4.08	3.76	5.48	4.92	
^1E	$5a_1 \rightarrow 8e$, $7e \rightarrow 3a_2$	$A(x,y)$	5.88	5.56	6.71	6.60	
$^1B_2$	$3b_1 \rightarrow 3a_2$	A(z)	6.00				
$^1B_1$	$4b_2 \rightarrow 3a_2$, $5a_1 \rightarrow 4b_1$	F	6.26				
^1E	$5a_1 \rightarrow 8e$, $7e \rightarrow 3a_2$	$A(x,y)$	6.34	6.63	7.76	6.78	
$^1A_2$	$7e \rightarrow 8e$	F	6.72				
$^1B_1$	$5a_1 \rightarrow 4b_1$, $4b_2 \rightarrow 3a_2$	F	7.07				
$^1A_2$	$7e \rightarrow 8e$, $3b_1 \rightarrow 5b_2$	F	7.13				
^1E	$4b_2 \rightarrow 8e$, $7e \rightarrow 4b_1$	$A(x,y)$	7.43				
^1E	$4b_2 \rightarrow 8e$, $7e \rightarrow 4b_1$	$A(x,y)$	7.51				
$^1B_2$	$7e \rightarrow 8e$, $3b_1 \rightarrow 3a_2$	$A(z)$	7.67				

[a]Singlet state contributing configurations are from Ref. 7 and represent excitation of a single electron from the first orbital to the second orbital.
[b]A stands for allowed and F for forbidden. The symbols x, y, z in parentheses after the A indicate the polarization of the corresponding transition. The O_Z axis is the C_2 symmetry axis of the COT molecule perpendicular to the plane of four of its carbon atoms, and the other two axes are in the two molecular symmetry planes and are perpendicular to O_Z.
[c]Reference 7.
[d]Reference 6.
[e]Reference 5.
[f]Reference 13.
[g]Reference 14 provides $S_0 \rightarrow T_1$ energy for COT in planar configuration. This energy has been increased by the inversion energy of the COT ring (0.18 eV) from Ref. 6.

5.06 eV, which wasn't, however, detected in subsequent optical studies.[5,6] The trapped electron spectrum,[13] which measures a quantity proportional to the integral of the scattering cross section over a narrow energy band above the threshold energy, shows a broad peak from approximately 2.7 to 5.8 eV with several smaller peaks superimposed upon it. Several stronger transitions are observed between 5.8 and 10 eV. The features observed between 3.4 and 4.2 eV were assigned in that study to singlet – triplet transitions.

III. EXPERIMENTAL

The apparatus used in this study has previously been described in detail.[17,18] The low-energy, variable-angle, electron-impact spectrometer consists basically of an electron gun which injects a collimated beam of thermionically emitted electrons into a hemispherical electrostatic energy monochromator with a mean radius of 2.54 cm. The energy-selected electron beam scatters off the target gas contained in a flexible bellows scattering chamber, and the scattered electrons are energy-analyzed by a second analyzer identical to the monochromator. A Spiraltron (continuous dynode) electron multiplier serves as the detector, and the output pulses are amplified, shaped, and stored in a 1024-channel multichannel scaler. In a typical experiment, the incident electron energy and scattering angle are both fixed, and the energy-loss spectrum is scanned repeatedly, usually for a period of 4–8 h. The energy-loss spectrum thus obtained is analogous to an optical absorption spectrum, except that optically forbidden processes are much more readily detected.[17–19] For each impact energy, the scattering angle is then changed and the procedure repeated.

The method of low-energy, variable-angle, electron-impact spectroscopy has been used successfully to investigate spin-forbidden and other electric dipole-forbidden transitions in molecules.[17–19] Information about the nature of the excited electronic states observed in an electron-impact spectrum can be obtained by studying the dependence of the scattering intensity of each transition on impact energy and angle.[17,19] Transitions which in optical spectroscopy are both electric dipole and spin-allowed, have, at impact energies of 15 eV or more above threshold, electron impact differential cross sections (DCS's) which are forward peaked, decreasing by approximately 2 orders of magnitude as the scattering angle varies from 10° to 80°.[17,19] In contrast, transitions involving changes in the molecular spin quantum number of unity, such as singlet – triplet excitations, have a more isotropic DCS (varying by less than about a factor of 3) over the angular range 10° to 80°. Such

transitions occur by the mechanism of electron exchange.[20] Spin-allowed but electric-dipole forbidden processes are forward peaked, but often not as much as fully allowed transitions.[17-19,21] Finally, for impact energies about 15 eV or more above threshold, optically forbidden processes, and in particular spin-forbidden ones, become more intense with respect to optically allowed ones as the impact energy is lowered.

In the present experiments, the electron energy-loss spectrum of COT vapor was studied at impact energies, E_0, of 30, 50, and 75 eV at scattering angles, θ, from 5° to 80°. Sample pressures in the scattering chamber ranged from 2 to 4 mTorr, as indicated by an uncalibrated Schulz-Phelps ionization gauge, while the electron beam current incident into the scattering chamber was approximately 60 nA. The energy resolution, as measured by the full width at half-maximum (FWHM) of the elastically scattered peak was electron-optically set in the range 0.10 to 0.13 eV. In these studies, two different samples of COT were used. One was obtained from the Aldrich Chemical Co. and has a specified purity of 98%, while another one was supplied by Professor Rowland Pettit of the University of Texas at Austin. Spectra obtained from both of these samples were identical. These samples were subjected to several liquid nitrogen freeze-pump-thaw cycles prior to use. When irradiated with a mercury vapor lamp COT is known to undergo various photochemical reactions including photoisomerization, decomposition into benzene and acetylene, and formation of styrene.[22] In order to minimize the possibility of these undesirable reactions the samples were protected from room light.

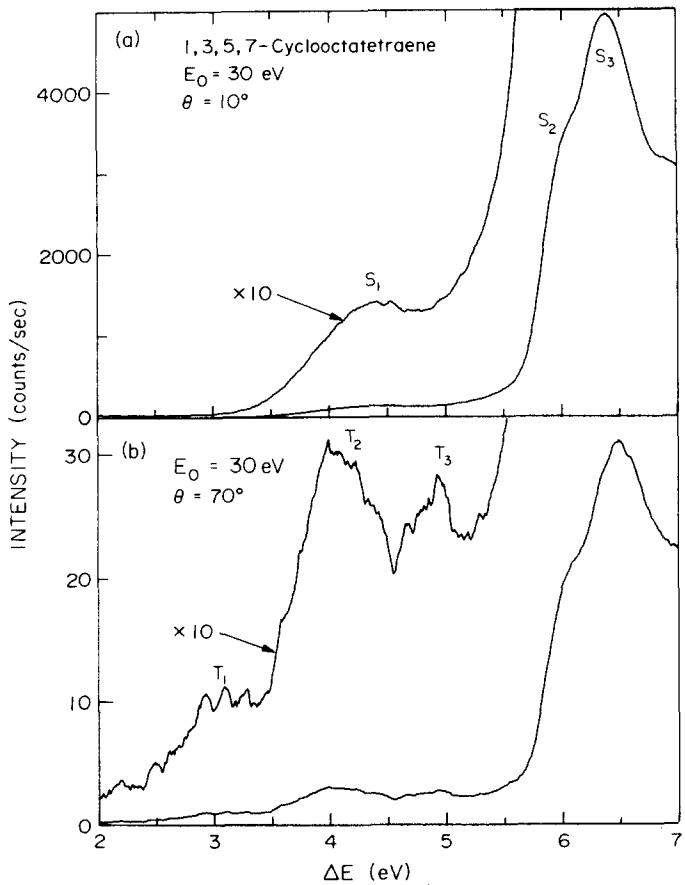

FIG. 1. Electron energy-loss spectrum of COT at (a) $\theta = 10°$ and (b) $\theta = 70°$; 30 eV incident energy; 5×10^{-8} A incident beam current; 4×10^{-3} torr sample pressure reading from an uncalibrated Schulz-Phelps gauge; resolution approximately 0.15 eV FWHM.

IV. RESULTS AND DISCUSSION

Figure 1 shows the 2 to 7 eV energy loss region of the COT electron impact spectrum at 30 eV impact energy and scattering angles of 10° and 70°. DCS values at impact energies of 30 and 50 eV are presented in Figs. 2 and 3. The elastic DCS's in arbitrary units were determined by multiplying the observed count rates by the scattering volume correction[23] appropriate for each scattering angle and normalizing the results to an arbitrary value of 1.0 at $\theta = 40°$. The reproducibility of these elastic DCS values is about ±20%.

The sum of the DCS's of the two transitions at 6.02 and 6.42 eV (designated S_2 and S_3, respectively) was obtained by multiplying the ratio of the area under the corresponding peak to that of the elastic peak (as previously described)[18,24] by the elastic DCS at each θ. In addition, for scattering angles of 30° and below, the combined DCS of these transitions was determined without reference to the elastic peak using the same procedure as for the elastic DCS, except that the DCS at 20° was normalized to the value obtained by the ratio (to the elastic DCS) method at this angle. These two methods gave results within 6% of one another at 30°.

The DCS curves for the other inelastic features displayed in Figs. 2 and 3 were determined by the ratio method using the elastic DCS as a reference for angles of 20° and above, and the $S_2 + S_3$ DCS below 20°. The estimated uncertainty in the inelastic DCS's is ±35%. The arbitrary units in Figs. 2 and 3 are the same for all curves at a given impact energy but differ from those of a different impact energy.

A. Triplet states

The lowest observed feature in the COT spectrum (Fig. 1) has an apparent onset at approximately 2.2 eV and an intensity maximum at 3.05 ± 0.05 eV. The DCS values for this transition at 50 eV impact energy do not vary by more than a factor of 3 over the angular range 20° to 80°. At 10° this feature is quite weak and contributions from the tails of adjacent transitions make it impossible to obtain an accurate DCS value. At an impact energy of 30 eV the DCS of this 3.05 eV electronic band varies by less than a factor of 2 over the angular range 10° to 80°. This behavior is indicative of a singlet – triplet transition and we designate it as $S_0 - T_1$. The lowest singlet – singlet transition occurring with a maximum intensity at 4.43 eV, is assigned as $\tilde{X}\,^1A_1 - {}^1A_2$ (see Sec. IV.B) The $S_0 - T_1$ transition probably corresponds, therefore, to the $\tilde{X}\,^1A_1 - {}^3A_2$ excitation. The lowest singlet – triplet transition reported by Knoop *et al.*,[13] using a trapped electron technique, at 3.4 eV is not in good agreement with our studies.

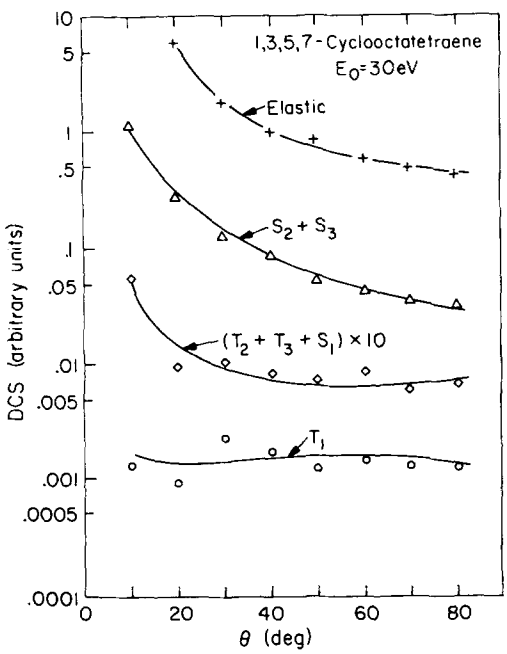

FIG. 2. Differential cross sections as a function of θ at an incident energy of 30 eV for elastic scattering (+) and for transitions to the following states: T_1(○), $(T_2+T_3+S_1)\times10$(◇), and S_2+S_3(△).

In addition to the $\tilde{X}\,^1A_1 - {}^1A_2(S_0-S_1)$ transition occurring at 4.43 eV, which is apparent at low scattering angles (Figs. 1a and 4), two other excitations are observed in this energy-loss region at larger scattering angles, occurring at 4.05 and 4.84 eV. These transitions are not visible at 10° and 20° (Figs. 1a and 4) due to the high intensity of the $\tilde{X}\,^1A_1 - {}^1A_2$ transition. However, at scattering angles of 40° and higher the DCS of this singlet – singlet transition has decreased so significantly that it is not clearly discernible, thereby making the transitions at 4.84 and 4.05 eV fully visible. These three transitions overlap each other appreciably and it is not possible to obtain accurate individual DCS values. Instead, the aggregate DCS for the energy-loss region from 3.4 to 5.4 eV has been plotted in Figs. 2 and 3 as the curve labeled $(T_2+T_3+S_1)$. At 50 eV impact energy this DCS decreases by less than a factor of 2 over the angular range 30° to 80° (compared to the S_2+S_3 DCS which decreases by a factor of 8 over the same angular range). Between 20° and 30° the 50 eV $(T_2+T_3+S_1)$ DCS decreases by a factor of approximately 4. This yields a total variation of about a factor of 5 over the angular range 20° to 80°. If only 50% of the aggregate intensity at 20° is due to the $\tilde{X}\,^1A_1 - {}^1A_2$ excitation, the two other transitions vary by a factor of 2.5 over the angular region 20° to 80°. This variation is most likely due to a singlet – triplet transition. The 50% contribution of the $\tilde{X}\,^1A_1 - {}^1A_2$ is probably an underestimate, since the transitions at 4.05 and 4.84 eV are no longer distinguishable at the 20° scattering angle.

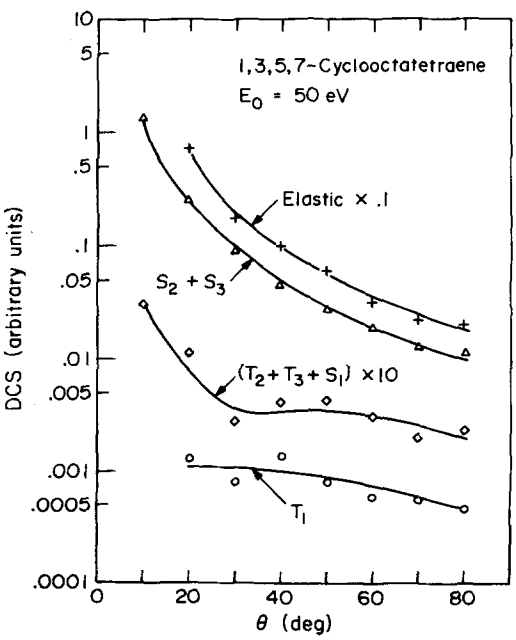

FIG. 3. Same as Fig. 2 for an incident energy of 50 eV. The elastic DCS has been multiplied by 0.1 before plotting.

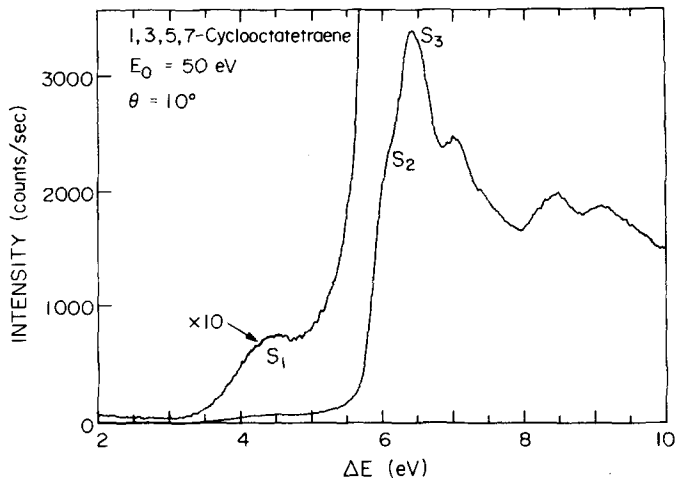

FIG. 4. Electron energy-loss spectrum of COT at $\theta = 10°$, 50 eV incident beam energy; 7×10^{-8} A incident beam current; 3×10^{-3} torr sample pressure reading from an uncalibrated Schulz–Phelps gauge; resolution approximately 0.15 eV FWHM.

When the impact energy is lowered to 30 eV, the contributions of the transitions at 4.05 and 4.84 eV are more pronounced, the aggregate DCS varying by less than a factor of 2 over the angular range 20° to 80°. On the basis of these data it is possible to identify the transitions at 4.05 and 4.84 eV as singlet – triplet excitations and designate them $S_0 - T_2$ and $S_0 - T_3$. These results are again not in good agreement with the trapped electron spectrum of Knoop *et al.*[13] As shown in Table II, they report additional triplet states at 3.7, 3.9, and 4.1 eV, while a singlet state was reportedly observed at 4.82 eV.

B. Singlet states

Figure 4 shows the COT spectrum at 50 eV impact energy and a scattering angle of 10°. At this energy and angle the contribution of singlet – triplet transitions to the spectrum should be small and the observed tran-

TABLE II. Summary of experimental observations of transition energies.

Nature of transition	Possible upper state	Energy of transition (eV) Optical[a]	Trapped electron[b]	Present study[c]
Singlet → triplet	or $^3A_2$	•••	3.4	3.05
Singlet → triplet	or ^3E	•••	3.7	4.05
Singlet → triplet	^3E	•••	3.9	4.84
Singlet → triplet	•••	•••	4.1	•••
Symmetry forbidden singlet → singlet	$^1A_2$	4.39	4.4	4.43
Electric dipole allowed singlet → singlet	^1E	6.05[d]	5.88	6.02[d]
Electric dipole allowed singlet → singlet	^1E	6.42		6.42
Electric dipole allowed singlet → singlet	^1B			6.99
Electric dipole allowed singlet → singlet	^1E			8.41
Electric dipole allowed singlet → singlet	^1E			9.05
Superexcited state	Rydberg State			10.2
Superexcited state				10.6
Superexcited state				11.3
Superexcited state				12.2
Superexcited state				14.2

[a]Reference 6.
[b]Reference 13.
[c]The accuracy of the transition energies below 9.1 eV is ±0.05 eV and those for the superexcited states is ±0.1 eV.
[d]Feature appears as a shoulder.

sitions may be considered to be essentially singlet → singlet excitations.

Batich *et al.*[4] found that a parameterization of the molecular orbital energies based on a simple Hückel model agreed quite well with the observed photoelectron spectrum. This is surprising because not only does the HMO model assume complete σ–π separation in this nonplanar system but it also neglects through-space interactions between the opposite π orbitals. Batich *et al.*[4] believe that the satisfactory parameterization of their experimental results "is due to compensation of through-space interactions across the ring by through-bond interactions with the lower lying σ orbitals." We have attempted to analyze the singlet → singlet excitation spectrum of COT in a similar manner.

The orbital ordering resulting from a Hückel calculation among the 8 $p\pi$ orbitals is shown in Fig. 5. In addition the highest energy occupied σ orbital, is also included. Energy spacings have been labeled α, β, γ, and δ as indicated in the figure. An approximate spacing of levels may be obtained from the photoelectron spectrum[4] (vertical IP's 8.47, 9.78, 11.15, and 11.55 eV) by applying Koopmans' theorem.[25] Using the ionization potentials of that spectrum we obtain for β, γ, and δ the values 1.31, 1.37, and 0.40 eV, respectively. We also set α equal to the vertical excitation energy of the $\tilde{X}\,^1A_1 \rightarrow {}^1A_2$ transition, 4.43 eV. Considering only the symmetry-allowed transitions the following excitations are expected (orbital occupancy changes are given in parentheses): two transitions of the type $\tilde{X}\,^1A_1(4b_2^2 7e^2 5a_1^2) \rightarrow {}^1E(4b_2^2 7e^2 5a_1^1 8e^1$ and $4b_2^2 7e^1 5a_1^2 3a_2^1)$ at 5.69 eV, one $\tilde{X}\,^1A_1 \rightarrow {}^1B_2(4b_2^2 7e^1 5a_1^2 8e^1)$ at 7.00 eV, and

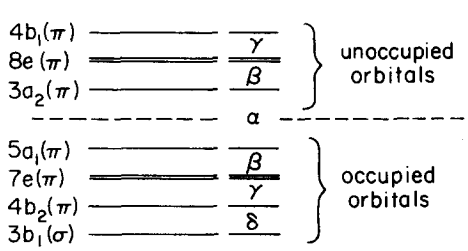

FIG. 5. COT valence orbital ordering. Orbitals below the dashed line are occupied in the ground state. The greek letters represent the energy spacing between the adjacent orbital levels. The ordering of occupied orbitals matches *ab initio* calculations of Lehn and Wipf while energy spacing is obtained via Koopman's theorem. The ordering and spacing of the virtual orbitals was obtained from a Hückel calculation and the energy spacing of the occupied orbitals. $\alpha = 4.43$ eV ($\tilde{X}\,^1A_1 \rightarrow {}^1A_2$ transition energy), $\beta = 1.31$ eV, $\gamma = 1.37$ eV, and $\delta = 0.40$ eV.

two $\tilde{X}\,^1A_1 \rightarrow {}^1E$ transitions ($4b_2^1 7e^2 5a_1^2 8e^1$ and $4b_2^2 7e^1 5a_1^2 4b_1^1$) at 8.37 eV. In addition the degenerate sets of E states at 5.69 and 8.37 eV would be expected to interact and split thereby breaking their degeneracy.[26,27] We now associate these transitions with the observed spectrum.

Figure 4 shows the $\tilde{X}\,^1A_1 \rightarrow {}^1A_2$ transition at 4.43 eV and a strong absorption beginning at about 5.5 eV. A strong feature can be seen with an intensity maximum at 6.42 eV, having a shoulder at 6.02 eV. These values are in good agreement with previously reported optical results.[6] We believe the shoulder and peak correspond to the lower split set of E states. This assignment, besides qualitatively agreeing with the Hückel parameterization, is in good agreement with the semiempirical calculation of Van-Catledge[7] who reports excitation energies of 5.88 and 6.34 eV. The transitions at 6.02 and 6.42 eV (designated S_2 and S_3) overlap heavily with each other and individual DCS's could not be obtained. The aggregate DCS for these transitions decreases by a factor of about 130 at 50 eV impact energy as the scattering angle increases from 10° to 80°, while the relative intensities of the two E states remain approximately the same. At 30 eV impact energy a factor of 34 decrease in the DCS is observed over the same angular range. The sharply forward peaked behavior of this DCS is characteristic of the symmetry-allowed singlet → singlet nature of these transitions.[17-19]

At 6.99 eV another transition is observed. This excitation may be tentatively assigned as the $\tilde{X}\,^1A_1 \rightarrow {}^1B_2$ transition predicted by our Hückel parameterization to occur at 7.0 eV. This energy does not agree too well with Van-Catledge's[7] calculated value of 7.67 eV for $\tilde{X}\,^1A_1 \rightarrow {}^1B_2$ transition. This transition could alternately be assigned as a $5a_1 \rightarrow 4s$ Rydberg transition with a reasonable term value of 11900 cm^{-1}.[28] It should be noted though, that we see no evidence of the $5a_1 \rightarrow 3s$ member of this series which would be expected near 5.2 eV,[29] or other transitions which could be assigned as higher members of this Rydberg series.

Two fairly intense transitions are observed at 8.41 eV and 9.05 eV, the latter being superexcited since it lies above the lowest I.P. of 8.47 eV. These transitions may be tentatively assigned as the two E states which we predicted above to lie at 8.5 eV by the Hückel parameterization. Complete DCS values were not obtained for these transitions; however, as would be expected for symmetry-allowed singlet → singlet transitions, their electronic band shapes relative to the lower E states change very little with respect to angle. The tentative nature of these latter assignments should be emphasized, as the corresponding transition energies calculated by Van-Catledge are 7.43 and 7.51 eV. The difference between these calculations and the experimental values could be due either to increasing inaccuracies in the semiempirical method as one moves to higher energies or to misassignments of the observed transitions. There is also the possibility that these two transitions are members of Rydberg series converging to ionization potentials higher than 8.47 eV. However, they do not appear to fall into any well-defined series.

In some of our spectra we observe a very weak transition at 7.4 eV which could be related to the $\tilde{X}\,^1A_1 \rightarrow {}^1B_2(\pi \rightarrow \pi^*)$ excitation. However, this transition may well be the $(3b_1^2 4b_2^2 7e^2 5a_1^2 \rightarrow 3b_1^1 4b_2^2 7e^2 5a_1^2 3a_2^1)\,\tilde{X}\,^1A_1 \rightarrow {}^1B_2$, $\sigma \rightarrow \pi^*$ excitation which is predicted to have a transition energy of 7.51 eV by the Hückel parameterization. Several other weak transition are observed with excitation energies above 10 eV. These transitions may be Rydberg superexcited states and their excitation energies are given in Table II.

V. COT'S ROLE IN DYE LASER QUENCHING

Flashlamp-pumped or cw dye laser operation has been found to be inhibited by the intersystem crossing of dye molecules from singlet to triplet manifolds.[8,9,30] Once the lowest triplet state of the dye is populated, triplet → triplet excitations can occur. It has been suggested that this process quenches lasing in a few microseconds.[9,31] For this reason, triplet state quenchers such as COT are added to the dye solution. They usually increase both the laser pulse length and its maximum pulse repetition rate.[11] In the case of rhodamine 6G (R6G) the maximum triplet → triplet absorption occurs at approximately 2.0 eV[32,33] which is in the region of laser emission of this dye.[33]

Using ESR techniques, Yamashita and Kashiwagi[12] found that at 77 °K COT effectively depopulated R6G's lowest triplet state. Dempster *et al.*[34] found the experimental rate constant for quenching, K_{exp}, of R6G by COT in ethanol solutions to be $(7 \pm 1) \times 10^8 M^{-1}\ sec^{-1}$. The exact mechanism of quenching, whether through direct triplet → triplet energy transfer of via complex (exciplex) formation, is unknown. Our results furnish information about this mechanism.

Dexter[35] has proposed a theoretical model for triplet → triplet energy transfer rates in crystals due to exchange interactions. The transition probability rate for energy transfer between the neighboring donor and acceptor in a crystal P_{da}^{cr} is given by

$$P_{da}^{cr} = \frac{2\pi}{\hbar} Z^2 \int f_d(E) F_a(E) dE, \tag{1}$$

where Z^2 is related to the Coulombic exchange integrals for the molecules, $f_d(E)$ is the normalized phosphorescence intensity distribution function of the donor (R6G), and $F_a(E)$ is the normalized singlet → triplet absorption intensity distribution function of the acceptor (COT). The value of $(2\pi/\hbar)Z^2$ may be estimated[35] to be approximately $1.0\ Y$ erg/sec. Y is a dimensionless constant related to the nodal characteristics of the wavefunction and is much smaller than unity. Gas phase studies by Schmidt and Lee,[36] involving π-bonded molecules indicate that the rate of triplet → triplet energy transfer is indeed proportional to the energy overlap of the donor molecule's phosphorescence spectrum with the $S_0 \rightarrow T_1$ absorption spectrum of the acceptor molecule. This overlap can be obtained either from direct or O_2-induced optical absorption measurements or from electron-impact spectroscopy.[18] This is consistent with Dexter's theoretical prediction for a crystal environment.

In attempting to estimate P_{da}^{cr} and subsequently the transition probability rate for solutions, P_{da}^{sol}, use may be made of our electron impact band shape for the $S_0 \rightarrow T_1$ transition in COT. The phosphorescence spectrum of R6G has been studied by Marling[37] but has not been published; its phosphorescence maximum occurs at 1.9 eV.[12] To estimate the spectral overlap we have assumed that the shape of the phosphorescence band is the same as that of the fluorescene intensity distribution of the lowest excited singlet state of R6G,[38] with its maximum shifted to 1.9 eV. The resulting overlap integral has the value of approximately 3×10^8 erg^{-1}, yielding a P_{da}^{cr} value of 3×10^8 Y sec^{-1}.

From this theoretical value of P_{da}^{cr}, we wish to obtain a rate constant for quenching in solution which can be compared to the experimentally observed one. P_{da}^{cr} may be related to P_{da}^{sol} by

$$P_{da}^{sol} = P_{da}^{cr}\{1 - ([s]/([A]+[s]))^n\}, \quad (2)$$

where n is the total number of solvent plus quencher molecules surrounding each donor molecule in solution, [A] is the concentration of the acceptor and [s] that of the solvent. The factor multiplying P_{da}^{cr} is an estimate of the fraction of the time that the donor has at least one acceptor molecule next to it in solution. Because the solvent is in great excess we may simplify (2) to

$$P_{da}^{sol} = P_{da}^{cr} n[A]/[s]. \quad (3)$$

P_{da}^{sol} is related to the triplet quenching rate equation by

$$-(1/[D])(d[D]/dt) = P_{da}^{sol} = K[A], \quad (4)$$

where [D] is the concentration of excited triplet donor. Using Eqs. (3) and (4), the theoretical rate constant is given by $K_{th} = P_{da}^{cr} n[s]^{-1}$. For the R6G–COT system in ethanol this results in a K_{th} value of 6×10^8 Y M^{-1} sec^{-1} (where n was estimated to be approximately 40 on the basis of size considerations).

Remembering that $Y \ll 1$, the theoretical rate constant is significantly smaller than the experimental rate constant of 7×10^8 M^{-1} sec^{-1}. While our method of estimation is admittedly crude, we feel that the difference in the orders of magnitude of the theoretical and experimental rate constants for quenching suffices to indicate the existence of another quenching mechanism beside direct triplet → triplet energy transfer. A reasonable second mechanism appears to be complex (or exciplex) formation.[39] The intimate interactions between molecules during the complex formation with the concurrent distortion of molecular geometries and possible changes in excited state energies provide another reasonable quenching mechanism. It is also interesting to compare the experimental triple quenching rate constant with the theoretical diffusion-limited value,[40] K_{dif}, of 8.8×10^9 M^{-1} sec^{-1} obtained from the viscosity of ethanol. K_{dif} is about ten times greater than K_{exp}, which implies that each encounter of a triplet R6G molecule with a COT molecule does not result in deactivation of the R6G.

VI. SUMMARY AND CONCLUSIONS

The transition energies determined in this study are summarized in the last column of Table II. Optically undetected excitations to three low-lying triplet states were observed at 3.05, 4.05, and 4.84 eV (positions of band intensity maxima). The lowest of these overlaps with the lowest triplet phosphorescence band of rhodamine 6G suggesting that it plays an important role in quenching the rhodamine 6G triplet. A theoretical estimate of the rate constant for this quenching by direct triplet → triplet energy transfer leads to a value too low to account for the experimentally observed one, suggesting that exciplex formation may play an important role in the quenching mechanism. Several singlet → singlet transitions have been observed in the energy-loss region of 4 to 10 eV. The excitations above 7 eV have not been previously detected. Several superexcited states were identified in the 10 to 15 eV energy-loss region.

ACKNOWLEDGMENTS

We wish to thank Professor R. Pettit for providing us with one of our samples of 1,3,5,7-cyclooctatetraene. We also thank Dr. W.M. Flicker for several very helpful discussions.

[1] M. Milun, Z. Sobotka and N. Trinajstic, J. Org. Chem. **37**, 139 (1972).
[2] M. Traetteberg, Acta Chem. Scand. **20**, 1724 (1966).
[3] O. Bastiansen, L. Hedberg, and K. Hedberg, J. Chem. Phys. **27**, 1311 (1957).
[4] C. Batich, P. Bischof, and E. Heilbronner, J. Electron Spectrosc. Relat. Phenom. **1**, 333 (1972/73).
[5] N. Allinger, J. Chow Tai, and T. Stuart, Theor. Chim. Acta **8**, 101 (1967).
[6] N. Allinger, M. Miller, L. Chow, R. Ford, and J. Graham, J. Am. Chem. Soc. **87**, 3430 (1965).
[7] F. Van-Catledge, J. Am. Chem. Soc. **93**, 4365 (1971).
[8] R. Pappalardo, H. Samelson, and A. Lempicki, Appl. Phys. Lett. **16**, 267 (1970).
[9] J. Marling, D. Gregg, and L. Wood, Appl. Phys. Lett. **17**, 527 (1970).
[10] J. Marling, L. Wood, and D. Gregg, IEEE J. Quantum Electron. **7**, 498 (1971).
[11] J. Weber, Z. Angew. Phys. **31**, 7 (1971).
[12] M. Yamashita and H. Kashiwagi, J. Phys. Chem. **78**, 2006 (1974).
[13] F. Knoop, J. Kistemaker, and L. J. Oosterhoff, Chem. Phys. Lett. **3**, 73 (1969).
[14] N. Baird, J. Am. Chem. Soc. **94**, 4941 (1972).
[15] *U. V. Atlas of Organic Compounds* (Butterworths, London, 1966), Vol. 1.
[16] A. Cope and C. Overberger, J. Am. Chem. Soc. **70**, 1433 (1948).
[17] (a) A. Kuppermann, J. K. Rice, and S. Trajmar, J. Phys. Chem. **72**, 3894 (1968); (b) J. K. Rice, Ph.D. thesis, California Institute of Technology, Pasadena, California, 1969.
[18] O. A. Mosher, W. M. Flicker, and A. Kuppermann, J. Chem. Phys. **59**, 6502 (1973).
[19] S. Trajmar, J. K. Rice, and A. Kuppermann, Adv. Chem. Phys. **18**, 15 (1970).
[20] J. R. Oppenheimer, Phys. Rev. **32**, 361 (1928).
[21] D. C. Cartwright, W. J. Hunt, W. Williams, S. Trajmar, and W. A. Goddard III, Phys. Rev. A **8**, 433 (1927).
[22] I. Tanaka and M. Okuda, J. Chem. Phys. **22**, 1780 (1954).
[23] S. Trajmar, D. C. Cartwright, J. K. Rice, R. T. Brinkmann, and A. Kuppermann, J. Chem. Phys. **49**, 5464 (1968).
[24] O. A. Mosher, W. M. Flicker, and A. Kuppermann, Chem. Phys. Lett. **19**, 332 (1973).
[25] T. Koopmans, Physica (The Hague) **1**, 104 (1934).

[26]G. Herzber, *Electronic Spectra of Polyatomic Molecules* (Van Nostrand, Princeton, 1967) p. 403.
[27]M. Tinkham, *Group Theory and Quantum Mechanics* (McGraw-Hill, New York, 1964) p. 221.
[28]M. B. Robin, *Higher Excited States of Polyatomic Molecules* (Academic, New York, 1974) Vol. I, p. 51.
[29]For a Rydberg term value, $R/(n-\delta)^2$, of 11,900 cm^{-1} for the $n=4$ transition, the quantum defect, δ, is found to be 0.97. Excitation energies, E, for other members of the Rydberg series may be predicted by use of the formula $E = \text{I.P.} - R/(n-\delta)^2$.
[30]*Dye Lasers, Topics in Applied Physics, Vol* 1, edited by F. P. Schäfer (Springer, New York, 1973) pp. 3 and 87.
[31]P. P. Sorokin, J. R. Lankard, V. L. Moruzzi, and E. C. Hammond, J. Chem. Phys. **48**, 4726 (1968).
[32]V. I. Tomin, B. A. Bushuk, and A. N. Rubinov, Opt. Spectrosc. **32**, 527 (1972).
[33]A. V. Aristov and Yu. S. Maslyukov, Opt. Spectrosc. **35**, 660 (1973).
[34]D. N. Dempster, T. Morrow, and M. F. Quinn, J. Photochem. **2**, 343 (1973/74).
[35]D. L. Dexter, J. Chem. Phys. **21**, 836 (1953).
[36](a) M. W. Schmidt and E. K. C. Lee, J. Am. Chem. Soc. **90**, 5919 (1968); (b) **92**, 3579 (1970).
[37]J. B. Marling, Ph.D. thesis, University of California, 1971, cited in Ref. 12.
[38]M. J. Weber and M. Bass, IEEE J. of Quantum Electron. **5**, 175 (1969).
[39](a) I. H. Kochevar and P. J. Wagner, J. Am. Chem. Soc. **92**, 5742 (1970); (b) **94**, 3859 (1972).
[40]A. D. Osborne and G. Porter, Proc. R. Soc. London. Ser. A **284**, 9 (1965).